

Improved Gaussian self-consistent method | Applications to homopolymers with different architectures in dilute solution

Edward G. Timoshenko

Theory and Computation Group, Department of Chemistry, University College Dublin, Belfield, Dublin 4, Ireland

Yuri A. Kuznetsov

Centre for High Performance Computing Applications, University College Dublin, Belfield, Dublin 4, Ireland
(April 14, 2024)

A version of the Gaussian self-consistent (GSC) method, which avoids the use of the Edwards' virial expansion, is presented. Instead, the mean energy is evaluated directly via a convolution of the attractive part of the pairwise non-bonded potential with the Gaussian trial radial distribution function. The hard sphere repulsion is taken into account via a suitably generalised Camahan-Starling term. Comparison of the mean-squared intermonomer distances and radius of gyration, as well as of the mean energy, between the results from the GSC calculations and Monte Carlo (MC) simulation in continuous space are made across the coil-to-globule transition for isolated ring, open and star homopolymers of varied lengths and flexibility. Importantly, both techniques utilise the same polymer model so that the data points could be directly superimposed. A surprisingly good overall agreement is found between these GSC and MC results. Caveats of the Gaussian technique and ways for going beyond it are also discussed.

PACS numbers: 36.20.-r, 36.20.Ey, 61.25.Hq

I. INTRODUCTION

The Gaussian self-consistent (GSC) method represents a quite general, albeit relatively simple, theoretical framework for studying the equilibrium, dynamics and kinetics of conformational changes in polymer solutions. One of its most attractive features is that it can be applied to virtually any type of heteropolymer^{1,3}, with any specific interaction terms involving e.g. chain stiffness^{4,5} or charges⁶. The connectivity of the chain can be arbitrary: an open polymer⁷, a ring⁸, a star⁹, or a dendrimer¹⁰, whether in the limit of a single chain¹¹ or at finite concentrations¹². Moreover, not only the radius of gyration of the polymer or the total density can be computed, but much finer details of the conformational structure, such as the mean-squared distances between monomers or radial distributions at a given time, are available. Such a versatility naturally comes at the cost of certain limitations and inaccuracies intrinsic to the technique. However, these are well known and manageable, although often largely overstated in the popular view. Some of these, such as the Gaussian shape of the radial distribution function (RDF), are quite unavoidable at the level of the GSC theory, but others, such as the traditional use of the Edwards' virial expansion^{13,14}, can indeed be surpassed as we shall demonstrate in the current work. This would permit us for the first time to compare observables between the predictions of the GSC technique and Monte Carlo (MC) simulation in continuous space based on the same model for given values of thermodynamic parameters throughout the range of the coil-to-globule transition.

Historically, perhaps the first of the equilibrium versions of the Gaussian method in application to a single homopolymer chain were independently proposed by S. Edwards et al¹⁵ and J. des Cloizeaux¹⁶. The approach of the work by Edwards¹⁵ relied on the following idea. One would like to approximate the coordinates of the real homopolymer chain, X_i , governed by the Gibbs distribution with the exact Hamiltonian H , via a 'trial' Gaussian chain with the monomer positions $X_i^{(0)}$, governed by a simpler trial Hamiltonian $H^{(0)}$. By assuming that the quantities $X_i = X_i - X_i^{(0)}$ and $H = H - H^{(0)}$ are small and hence by applying the Taylor expansion to the equilibrium Gibbs averages, in the first order, one requires that the mean-squared radius of gyration obeys,

$$\langle R_g^2 \rangle = \langle R_g^{(0)2} \rangle; \text{ or equivalently } \langle R_g^{(0)2} H^{(0)} \rangle - \langle R_g^{(0)2} \rangle \langle H^{(0)} \rangle = 0: \quad (1)$$

Corresponding author. Web: <http://darkstar.ucd.ie>; E-mail: Edward.Timoshenko@ucd.ie

Such a theory predicts the correct mean-field swelling exponent $\nu_F = 3/5$ for the repulsive coil, only missing the subtle renormalisation group correction. It also gives appropriately $\nu = 1/2$ for the ideal coil, and $\nu_g = 1/3$ for the globule. Moreover, this approach can be further extended to kinetics by considering time dependent analogues of Eq. (1)^{17;18;18}.

A seemingly more refined theory proposed by des Cloizeaux¹⁶ uses $N-1$ (where N is the degree of polymerisation) variational variables $X_q^{(0)}$, which are the normal modes of the monomer positions for a ring chain $X_i^{(0)}$. This technique is based on the standard Gibbs-Bogoliubov variational principle with a quadratic diagonal trial Hamiltonian $H^{(0)}$. The equilibrium corresponds to the minimum of the trial free energy, $A_{\text{trial}} = A^{(0)} + \langle H - H^{(0)} \rangle_{i_0}$, where $A^{(0)}$ is the free energy associated with $H^{(0)}$. Expressed in the Edwards' form the extremum conditions for the trial free energy are precisely the following $N-1$ equations,

$$\langle H X_q^{(0)} \rangle_{i_0} = \langle H X_q^{(0)} \rangle_{i_0}; \quad \text{or equivalently} \quad \langle H X_q^{(0)} \rangle_{i_0} - \langle H X_q^{(0)} \rangle_{i_0} = 0: \quad (2)$$

Unfortunately, this theory, although more accurate for polymers around the theta-point and indeed for the globule, is known to have a deficiency in that it predicts the exponent $\nu = 2/3$ instead of the mean-field value of $\nu_F = 3/5$ for the swollen coil in the thermodynamic limit $N \rightarrow \infty$. For this reason, some suspicion arose concerning the validity of the theory by des Cloizeaux, hampering further efforts in this direction. It should be emphasised, however, that for finite values of N the resulting theory does give quite reasonable numerical results fairly close to $\nu_F = 3/5$. In fact, the numerically fitted value of the swelling exponent tends to be somewhere in between the two above theoretical predictions. In a way, this is not an unusual situation, even for the more elaborate integral equations theories of molecular fluids used in attempts to deduce the Flory exponent^{19;20}. More importantly, this well known deficiency of the theory by des Cloizeaux becomes irrelevant when considering the theta-point or the poor solvent conditions.

Therefore, activity on further extending and improving the GSC theory has persisted, notably in Milan by G. Allegra and F. Ganazzoli et al.^{21;5;3;2;22;23;10}, in Saclay by H. Orland and T. Garel et al.^{7;18;6}, as well as in our Group in Dublin^{8;7;1;4;11;12}, and some collaborations between these have emerged⁹. Furthermore, extensions of the GSC theory to kinetics, as well as to essentially any polymeric system, have been also achieved. For the former end, one proceeds from the Langevin equation and approximates the exact stochastic ensemble via a linear trial one. We refer the reader to our papers in Refs. 1,11,9 for the ultimate formulation of the GSC theory in terms of the real space variables. Such a version of the GSC method avoids the limitations of the earlier normal modes formulations since it can distinguish the frustrated states of heteropolymers with spontaneously broken kinematic symmetries associated with the connectivity structure.

Despite the relative success of the most recent form of the GSC method, the theoretical situation is not as yet fully satisfactory and further efforts along these lines are required. Firstly, one would like to be able to use the actual molecular interaction parameters rather than the coefficients in the Edwards' virial expansion, which are somewhat obscure in their meaning. Secondly, the convergence of such a virial expansion in the dense liquid globular state is rather problematic, being at best that of an asymptotic series. Thirdly, despite the conventional view, the three-body term is unable by itself to fully withstand a catastrophic pairwise collapse of monomers onto each other in the attractive regime for heteropolymers. In Refs. 1,11 an ad hoc self-interaction energy term has been added to tackle this problem, but it is merely a tweak of the model. Finally, the effective three-body and higher order virial terms make the current theory numerically inefficient due to a scaling law involving a high power in N for the time expense per step, despite the fact that the original model only contains two-body interactions.

Therefore, in the current work we shall rid ourselves of relying on the virial representation of the Hamiltonian entirely. Indeed, the exact molecular two-body potential can be averaged over the Gaussian RDF directly. However, the Gaussian function does not vanish at the origin, yielding a divergence from the repulsive part of the Lennard-Jones pairwise potential. One simple alternative is to use the latter potential with a hard core part, as in Ref. 24, in which case one has to cut off the integration at the hard sphere diameter, or more generally, within the excluded volume area.

To include the effect of the hard sphere repulsion one can in principle use any of the standard reference techniques developed for the hard sphere liquids, e.g. the Percus-Yevick expression for RDF, or the Camahan-Starling (CS) free energy formula^{25;26}. We prefer to use the latter due to its practical simplicity and accuracy when compared to molecular simulations. The Camahan-Starling equation, which was originally derived for a single component hard sphere liquid, has been naturally extended to mixtures. It is quite popular in the liquid matter literature at present (see e.g. Ref. 27). Its extension to polymeric fluids is somewhat less obvious though. Here we propose to express the partial packing coefficient for each of the monomers via an integral of the Gaussian trial RDF over the excluded volume area. The resulting GSC equations involve well tractable, albeit somewhat more complicated than before, expressions, since they now depend on the exact shapes of the molecular potentials.

Although we shall present the resulting technique in its most general form, which is applicable to any type of polymeric system, our numerical analysis in this work will be restricted by homopolymers of three different architectures

ring, open and star | across the coil to globule transition. This is done to enable us to make a comparison of the results from the present GSC theory with the MC data obtained in our previous paper in Ref. 24.

II. MODEL

The current coarse-grained polymer model is based on the following Hamiltonian (energy functional)^{24,49,28} in terms of the monomer coordinates, X_i :

$$\begin{aligned} \frac{H}{k_B T} = & \frac{1}{2} \sum_{i,j} \chi_{ij} (X_i - X_j)^2 + \frac{1}{2} \sum_{i,j,k} \chi_{ijk} (X_i + X_k - 2X_j)^2 \\ & + \frac{1}{2} \sum_{ij; i \neq j} \chi_{ij}^{(lj)} (X_i - X_j)^2 + U_{ij}^{(cou)} (X_i - X_j)^2 : \end{aligned} \quad (3)$$

Here the first term represents the connectivity structure of the polymer with harmonic springs of a given strength χ_{ij} , introduced between any pair of connected monomers (which is denoted by $i-j$). The second term represents the bending energy penalty given by the square of the local curvature with a characteristic stiffness χ_{ijk} between any three consecutively connected monomers (which is denoted by $i-j-k$) in the form of the Kratky-Harris-Hearst. Below we shall prefer to rewrite the first two terms in the following equivalent form,

$$\frac{H^{(bond)}}{k_B T} = \frac{1}{2} \sum_{ij} U_{ij}^{(bond)} (X_i - X_j)^2 : \quad (4)$$

Finally, the third and fourth terms represent pairwise non-bonded interactions between monomers such as the van der Waals and Coulomb forces. We can adopt the Lennard-Jones form of the former potential,

$$U_{ij}^{(lj)}(r) = \begin{cases} \infty & r < r_i^{(0)} + r_j^{(0)} \\ \frac{U_{ij}^{(0)}}{12} \left(\frac{r_i^{(0)} + r_j^{(0)}}{r} \right)^{12} - \frac{U_{ij}^{(0)}}{6} \left(\frac{r_i^{(0)} + r_j^{(0)}}{r} \right)^6 & r > r_i^{(0)} + r_j^{(0)} \end{cases} ; \quad (5)$$

where there is also a hard core part with the monomer radii $r_i^{(0)}$, and where $U_{ij}^{(0)}$ are the dimensionless strengths of the interactions. The Coulomb interaction potential similarly is,

$$U_{ij}^{(cou)}(r) = q_i q_j \frac{1}{r} \exp(-r/\lambda_D); \quad \lambda_D = \frac{Q_0^2}{4 \epsilon_0 k_B T}; \quad (6)$$

where λ_D is the Debye screening length, ϵ_0 is the dielectric permittivity of vacuum, $Q_i = Q_0 q_i$ are the charges, and λ_D is the Bjerrum length.

III. METHOD

A. Equations of the GSC method

The main objects in the GSC method are the mean-squared distances between monomers,

$$D_{ij}(t) = \frac{1}{3} \langle (X_i(t) - X_j(t))^2 \rangle : \quad (7)$$

Note that our convention includes the factor of $1/3$ here and hence in the later definition of the mean-squared radius of gyration according to the tradition. This allows us to rid of such factors from the radial distribution function (RDF) and numerical averages over it.

The GSC method is based on replacing the stochastic ensemble for X_i with the exact Hamiltonian in the Langevin equation of motion onto the trial ensemble $X_i^{(0)}(t)$ with a trial Hamiltonian $H^{(0)}(t)$. The latter is taken as a generic quadratic form with the matrix coefficients, which are called the time-dependent effective potentials,

$$H^{(0)}[X(t)] = \frac{1}{2} \sum_{ij} V_{ij}(t) X_i(t) X_j(t); \quad (8)$$

Then one requires that the intermonomer correlations satisfy the condition,

$$\langle X_i(t) X_j(t) \rangle_0 = \langle X_i^{(0)}(t) X_j^{(0)}(t) \rangle_0; \quad (9)$$

which means that the trial ensemble well approximates the exact one as far as monomer correlations are concerned. This procedure yields expressions for the effective potentials via the instantaneous mean energy,

$$V_{ij}(t) = \frac{2}{3} \frac{\partial E[D(t)]}{\partial D_{ij}(t)}; \quad (10)$$

and hence the mean squared distances themselves satisfy the self-consistent equations⁹. These, in the absence of the hydrodynamic interaction, are simply,

$$\frac{\gamma_b}{2} \frac{d}{dt} D_{ij}(t) = \frac{2}{3} \sum_k (D_{ik}(t) - D_{jk}(t)) \frac{\partial A[D(t)]}{\partial D_{ik}(t)} - \frac{\partial A[D(t)]}{\partial D_{jk}(t)}; \quad (11)$$

Here γ_b is the friction coefficient of a monomer, and the instantaneous free energy has the same functional expression via the instantaneous $D_{ij}(t)$ as it has at equilibrium. Extension to the preaveraged hydrodynamic approximation is quite straightforward also and it is discussed in Ref. 1.

The stationary limit of these equations produces the equations for the minimum of the free energy, which are the same as those derived from the Gibbs-Bogoliubov variational principle with a generic quadratic trial Hamiltonian. Although in this paper we shall only be concerned with the equilibrium properties, the numerical solution of Eq. (11), applied until the stationary limit is reached, presents by far the most efficient technique for finding the global free energy minimum. This, based on the fifth order adaptive step Runge-Kutta integrator¹, was used for obtaining the results from the GSC technique in this work.

It should be also noted that the systems studied here possess a large number of kinematic symmetries for D_{ij} , and hence for V_{ij} , matrices coming from their symmetry and from the equivalence of any monomer in a ring, or any arm in a star homopolymers. Thus, the computational expenses per step in our calculations are of order $t_c N^2$, where $N = 2 < F < N^2 = 2$ is the total number of independent elements in the matrix D_{ij} . These symmetries significantly reduce the computational times compared to MC for an equivalent system, where such symmetries only appear in the observables after averaging over the statistical ensemble. For comparison, the computational expenses per step in MC are of order $t_c N^2 S$, where $t_c N^2$ is the number of MC steps needed to ensure a good statistical independence between measurements, and where S is the number of measurements needed for sampling of observables. Typical values of S should be of order of $10^4 - 10^6$ for a good accuracy in the present case²⁴. Moreover, kinetic iteration of the GSC equations towards the equilibrium is also significantly faster than the equivalent equilibration procedure in the MC. For example, for a ring polymer of $N = 150$ units in the good solvent, $U^{(0)} = 1$, the GSC method turns out to be 1000 times faster²⁹ than MC for gaining the same data, whereas for an open chain of the same length, which possesses much fewer kinematic symmetries, GSC is 200 times faster than MC.

B. Hard sphere contribution

Camahan and Starling have devised a simple but rather accurate equation of state for hard sphere liquids²⁶ in terms of the packing coefficient, yielding the following free energy,

$$\frac{A^{(CS)}}{k_B T N} = F^{(CS)}(\eta) = \frac{(4 - 3\eta)}{(1 - \eta)^2}; \quad \eta = N \frac{v_0}{V}; \quad (12)$$

where v_0 and V are the volumes of the hard sphere and of the whole system respectively. This is obtained from an interpolation formula for the virial coefficients based on several of them known exactly (see more detailed discussions in e.g. Ref. 25).

To extend these ideas to polymeric fluids, we would have to distinguish the packing coefficients for individual monomers. In Eq. (12) we can write $N = N_i$; the volume of the sphere v_0 is equal to the 1/8-th of its excluded volume; and the inverse volume is equal to the RDF of the ideal reference system, $1/V = g_{ideal}^{(2)}$. Thus, we can similarly

express the packing coefficient for the i -th monomer as a sum over all other monomers of the 1=8-th of the integral over the excluded volume of the monomer i of the RDF for the Gaussian reference system,

$$g_{ij}^{(2)}(r) = \frac{1}{(2D_{ij})^{3/2}} \exp\left(-\frac{r^2}{2D_{ij}}\right); \quad (13)$$

yielding finally,

$$= N \frac{V_0}{V} \int \prod_{i \in j} \frac{a}{8} \int_{r > r_i^{(0)} + r_j^{(0)}}^Z dr g_{ij}^{(2)}(r); \quad (14)$$

One may note that the Gaussian distribution does not possess a well defined volume beyond which it vanishes. Thus, to account for this we can, in principle, include a multiplicative parameter a , which should be once and for all chosen to match the data best, but this should, in any case, be fairly close to the unity. Therefore, the total hard sphere contribution will be,

$$\frac{A^{(hs)}}{k_B T} = N F^{(CS)}(\cdot) \int \prod_i F^{(CS)}(\cdot_i); \quad (15)$$

C. Free energy in the GSC method

The total mean energy includes both the bonded and the pairwise nonbonded interactions via,

$$\frac{E^{(int)}}{k_B T} = \frac{1}{2} \sum_{ij} 3U_{ij}^{(bond)} D_{ij} + \sum_{r > r_i^{(0)} + r_j^{(0)}}^Z dr g_{ij}^{(2)}(r) [U_{ij}^{(lj)}(r) + U_{ij}^{(cou)}(r)]; \quad (16)$$

Note that here we integrate only beyond the excluded volume as the hard sphere contribution will be included explicitly via the Camahan (Starling) term.

Given that the conformational Gaussian entropy has been calculated by us in Appendix B of Ref. 1, the total free energy can be summarised as follows,

$$A = E - TS; \quad E = E^{(int)} + A^{(hs)}; \quad E^{(int)} = E^{(bond)} + E^{(lj)} + E^{(cou)}; \quad S = S^{(gau)}; \quad (17)$$

where its various terms are given by,

$$\frac{E^{(bond)}}{k_B T} = 3 \sum_{i < j} U_{ij}^{(bond)} D_{ij}; \quad (18)$$

$$\frac{E^{(lj)}}{k_B T} = \sum_{i < j} U_{ij}^{(0)} E^{(lj)} [Y_{ij}]; \quad (19)$$

$$\frac{E^{(cou)}}{k_B T} = \sum_{i < j} \frac{1}{r_i^{(0)} + r_j^{(0)}} E^{(cou)} [Y_{ij}; (r_i^{(0)} + r_j^{(0)}) = 1]; \quad (20)$$

$$\frac{S^{(gau)}}{k_B} = \frac{3}{2} \ln \det R^{(N-1)}; \quad (21)$$

$$\frac{A^{(hs)}}{k_B T} = \sum_i F^{(CS)}(\cdot_i); \quad F^{(CS)}(\cdot_i) = \frac{1}{(1 - \frac{3}{2} \cdot_i)^2}; \quad (22)$$

and the arguments of these functions are defined as,

$$\cdot_i = a \sum_{j \in i} F^{(1)} [Y_{ij}]; \quad (23)$$

$$Y_{ij} = \frac{\frac{1}{D_{ij}}}{r_i^{(0)} + r_j^{(0)}}; \quad (24)$$

$$R_{ij} = \frac{D_i + D_j}{2} R_g^2 \frac{D_{ij}}{2}; \quad D_i = \frac{1}{N} \sum_j D_{ij}; \quad R_g^2 = \frac{1}{2N^2} \sum_{ij} D_{ij}; \quad (25)$$

Finally, the functions of y_{ij} are,

$$F^{(1)}[y] = \frac{1}{(2y)^3} \int_0^{\frac{r}{2}} x^2 dx \exp\left(-\frac{x^2}{2y^2}\right) = \frac{y \operatorname{erf}\left(\frac{1}{y\sqrt{2}}\right)}{8y}; \quad (26)$$

$$E^{(1j)}[y] = \frac{1}{y^3} \int_0^{\frac{r}{2}} x^2 dx \exp\left(-\frac{x^2}{2y^2}\right) \frac{1}{x^{12}} = \frac{y \int_0^{\frac{1}{y\sqrt{2}}} \exp\left(-\frac{1}{2y^2}\right) dy}{945y^{12}} \frac{1 + 315y^6 \operatorname{erfc}\left(\frac{1}{y\sqrt{2}}\right)}{1 + 315y^6}; \quad (27)$$

$$E^{(cou)}[y; k] = \frac{1}{y^3} \int_0^{\frac{r}{2}} x^2 dx \exp\left(-\frac{x^2}{2y^2}\right) \frac{\exp(-kx)}{x} = \exp\left(-\frac{1}{2y^2}\right) k \int_0^{\frac{1}{y\sqrt{2}}} \frac{2k}{\exp\left(-\frac{(1+ky^2)^2}{2y^2}\right)} \operatorname{erfc}\left(\frac{1+ky^2}{y\sqrt{2}}\right) dy; \quad (28)$$

Here we have used the standard definitions for the error functions,

$$\operatorname{erf}(z) = \frac{2}{\sqrt{\pi}} \int_0^z \exp(-x^2) dx; \quad \operatorname{erfc}(z) = 1 - \operatorname{erf}(z); \quad (29)$$

Note also that for a large z , numerically, one has to use the truncated asymptotic expansion in calculating $E^{(cou)}$ to avoid divergences,

$$\operatorname{erfc}(z) \exp(z^2) = \frac{1}{z} - \frac{1}{2z^3} + \frac{3}{4z^5} - \frac{15}{8z^7} + \dots; \quad (30)$$

IV. RESULTS

Here we shall restrict ourselves by the case of homopolymers, so that in Eq. (3) all non{zero bonded interaction constants are equal: $u_{ij} = u$, $u_{ijk} = u$, as well as all non{bonded interaction parameters are identical in Eq. (5): $U_{ij}^{(0)} = U^{(0)}$, $r_1^{(0)} = d = 2$. We also choose the hard sphere diameter d equal to the length ℓ defined in Eq. (3), as in Ref. 24. Moreover, henceforth we shall use the mean energy $E^{(int)}$ expressed in units of $k_B T$ and the mean{squared distances D_{ij} and the mean{squared radius of gyration $3R_g^2$ expressed in units of ℓ^2 .

Firstly, to understand the influence of the adopted Camahan{Starling term, we shall look at the case of a ring homopolymer with varied values of the spring constant in the good atherm also solvent, $U^{(0)} = 0$. In Tab. I we compare values of the mean energy $E^{(int)}$ between MC and GSC with two choices of the multiplicative parameter a in Eq. (23) for the packing coefficient, namely $a = 0.9$ and $a = 1.0$. Likewise, in Tab. II we present the data for the mean{squared radius of gyration $3R_g^2$. One can see that the results from the GSC theory simply coincide with those from MC as $a \rightarrow 0$. Yet, the agreement in the energy is somewhat better for the theory with $a = 0.9$ than for that with the naive choice $a = 1.0$, and that is how exactly the particular value $a = 0.9$ has been chosen by us. A typical relative error in the energy is less than 1.5 percent for $a = 0.9$ and is under 4 percent for $a = 1.0$. The agreement for the mean{squared radius of gyration is somewhat less impressive — the relative error steadily increases with ℓ , being better for $a = 0.9$, but never exceeding a few dozen percent.

One can comment on the reason why a value $a < 1$ produces a somewhat better agreement with MC. To facilitate this discussion, RDFs from the GSC and MC techniques are exhibited in Fig. 1. In Ref. 24 we have discussed the role of the 'correlation hole' at small separations beyond the excluded volume area, which is also evident for $r < 1.5$ in the main part of Fig. 1. As this feature is absent in the Gaussian theory (see Eq. (13)), the resulting packing coefficient values in Eq. (23) are overestimated. Thus, reducing the parameter a permits us to effectively lower the packing coefficient and this can be done only once because the correlation hole effect is expressed in terms of the function of the dimensionless variables,

$$\hat{g}_{ij}^{(2)}(\hat{r}) = D_{ij}^{3/2} g_{ij}^{(2)}(r); \quad \hat{r} = \frac{r}{D_{ij}^{1/2}}; \quad (31)$$

Next, we would like to analyse the dependence on the degree of polymerisation, N , in the good solvent, $U^{(0)} = 0$, (the second block in Tabs. I, II). The mean energy in this case comes entirely from the bonded interactions and hence the relative energy deviation of G SC from M C does not increase with N . This means simply that the values of $D_{i,i+1}$ match with those from M C quite well. As for the radius of gyration, the disagreement increases slowly with N , i.e. the mean squared distances $D_{i,i+k}$ are increasingly more overestimated by G SC as compared to M C for large k . Based on these results, we can determine the swelling exponent of the ring coil by fitting $3R_g^2$ via Eq.,

$$3R_g^2 = b^2 N^2 \quad (32)$$

using our data in the range $N = 50 - 500$. The resulting prefactor b^2 and the exponent in all three cases are,

$$b^2 = \begin{array}{l} 8 \\ < 0.223 \quad 0.005 \quad \text{M C} \\ 0.180 \quad 0.003 \quad \text{G SC ; } a = 0.9 \\ : 0.184 \quad 0.003 \quad \text{G SC ; } a = 1.0 \end{array} \quad (33)$$

$$\begin{array}{l} 8 \\ < 0.610 \quad 0.006 \quad \text{M C} \\ = 0.648 \quad 0.002 \quad \text{G SC ; } a = 0.9 \\ : 0.651 \quad 0.001 \quad \text{G SC ; } a = 1.0 \end{array} \quad (34)$$

Thus, the increase in the deviation of $3R_g^2$ in the G SC method from M C indeed comes entirely from the overestimation of the swelling exponent. This is believed to reach the value $\nu = 2/3 = 0.666 \dots$ asymptotically. However, in the present range of N both G SC and M C give higher apparent exponent values than the most accurate renormalisation group result up to $\nu = 0.5882 - 0.0011$. The G SC results for ν are only slightly sensitive on the value of a , being in a relatively small overestimation over the M C results. This is related to the Gaussian shape of $g_{ij}^{(2)}$ in the G SC theory, whereas a stretched exponential tail, $\exp(-B/r)$, (see the range $r > 40$ in Fig. 1) contributes most to $3R_g^2$ in M C. We may note also that the G SC estimate for ν is fairly close to the result $\nu = 0.635$ from the integral equations approach based on a complicated closure of the Born-Green-Yvon hierarchy in Ref. 20.

When considering open flexible homopolymers ($\nu = 1$, $\nu = 0$) in the good solvent ($U^{(0)} = 0$), the general behaviour of $E^{(int)}$ and $3R_g^2$ in the third block of Tabs. I, II is very similar to that of a ring: a good and almost N -independent agreement for $E^{(int)}$ and a slow increase with N in the relative error for $3R_g^2$. In Fig. 2 we plot the mean squared distances from the end monomer D_{0k} vs the chain index k . Up to $k = 10$, the agreement of both G SC curves with the M C data is nearly perfect, whereas both G SC curves increasingly overestimate the M C data for larger k . This is consistent with the overestimation of $3R_g^2$ by the G SC method, dominated by large k contributions. Notably, the effect of changing the parameter a is rather weak on this scale.

Further, let us investigate the effect of increasing the chain stiffness from a value corresponding to a fairly flexible ring $\nu = 1$ (see Fig. 3 and the fourth block in Tabs. I, II) to that of a semiflexible ring $\nu = 5$ (see Fig. 4 and the fifth block in Tabs. I, II). The fairly flexible case gives the energies in a very good agreement with the M C data, albeit the theory with $a = 0.9$ is somewhat less accurate accidentally. However, the agreement of $3R_g^2$ in the G SC theory with M C is even better here than for the corresponding flexible coil. The semiflexible case also gives the energies in a good agreement with the M C data, while $3R_g^2$ tends to be underestimated by the G SC method. Plots of the mean squared distances D_{0k} vs the chain index k in Figs. 3, 4 match nearly perfectly up to $k = 10$ as well, diverging for larger k . The M C curve is lower (higher) than the G SC curves for $\nu = 1$ ($\nu = 5$) in accord with the tables data. Thus, overall, the increase of $3R_g^2$ with the chain stiffness is more rapid in M C than in the G SC theory. Indeed, conformations of a stiff chain in M C become those of a rigid ring (or rod for an open chain) with increasing ν . However, the Camahan-Starling equation was deduced in the assumption of a total 3-d isotropy, when its influence would be weaker than in an effective 1-d projection.

Next, let us bring our attention to the effect of changing the topology of the chain. Thus, in the sixth block of Tabs. I, II we present $E^{(int)}$ and $3R_g^2$ for the flexible ($\nu = 0$) stars with the arm length $N = f = 50$ in the good solvent ($U^{(0)} = 0$). The relative errors in $E^{(int)}$ and $3R_g^2$ increase with the number of arms f steadily, again the energy values being more close between M C and G SC. The mean squared distances D_{0k} from the core monomer for the largest star with $f = 12$ arms are plotted in Fig. 5. Clearly, the agreement between G SC and M C is the worst of all previously considered cases here. Even the values of D_{0k} do not match for small k because the core monomer is strongly affected by the very pronounced correlation hole effect in M C²⁴. However, D_{ij} between monomers within same arms and away from the core are naturally closer between G SC and M C, just as for the open chain in Fig. 2. Clearly, the divergence of the G SC and M C curves does not increase with k after $k = 10$ and the curves have rather similar overall shapes.

It is interesting to analyse the structure of the collapsed globule now. Thus, in Fig. 6 the mean squared distances D_{0k} are plotted vs k for a flexible ring homopolymer in the globular state, $U^{(0)} = 6$. Overall shapes of the G SC and M C curves are quite similar, reflecting the compactness of the globule. The discrepancy between G SC and M C at

small k is present systematically. GSC generally overestimates the values of all D_{0k} , but the theory with $a = 0.9$ manages to come to a nearly correct limit of the globule size for $k > 20$ (see Ref. 24), whereas the theory with $a = 1.0$ is less accurate. The data for $3R_g^2$ in the last block of Tab. II thus show a much better agreement than before, but the energy values in Tab. I have a significantly larger discrepancy between GSC and MC. The GSC theory noticeably underestimates the negative Lennard-Jones energy contribution between all pairs of monomers. This, however, is to be expected given that the shape of RDF from MC²⁴ has a very tall first liquid-like peak (see the inset of Fig. 1). Since the Lennard-Jones interaction is rather short-ranged, the first peak gives a predominant negative contribution to the mean energy in Eq. 16. As the GSC theory has merely an effective smooth 'interpolating' Gaussian in $q_{ij}^{(2)}$ in that area (see the inset of Fig. 1), the resulting negative energy contribution is significantly smaller in such a theory.

We can also remark that the scaling for the swelling exponent in the globule is correct in the GSC theory. Indeed, the maximal compression is reached when $\chi < 1$, therefore by considering $y_{ij} \rightarrow 1$ in Eqs. (23,24,26) we indeed obtain, $D_{ij} \propto (r_i^{(0)} + r_j^{(0)})^2 N^{2/3}$.

Next, we would like to look at the plots of the mean squared radius of gyration, $3R_g^2$, and of the mean energy, $E^{(int)}$ across the coil-to-globule transition. These are depicted in Figs. 7 and 8 respectively. The following points can be made. First of all, the shapes of these curves are quite similar for MC and GSC with both values of a . Secondly, the coil-to-globule transition is continuous in all three cases, with the energy slope changing noticeably at around the theta-point. Thirdly, the transition occurs at a somewhat higher value of the attraction constant $U^{(0)}$ in the GSC theory than in the MC simulation. This can be explained by the underestimation of the Lennard-Jones attraction energy in the globule discussed above. Lastly, $3R_g^2$ of the globule is partly overestimated by the GSC method with $a = 1$, since the value $U^{(0)} = 6$ is much closer to the point of the coil-to-globule transition for the theory with $a = 1$ than that with $a = 0.9$ or MC.

Finally, to understand the N -dependence of the coil-to-globule transition in Fig. 9 we present the plots of the specific energy slope, $N^{-1}dE^{(int)}/dU^{(0)}$, vs $U^{(0)}$ for the flexible rings of different sizes. These curves nearly coincide in the repulsive coil region, starting to diverge from a value of $U^{(0)} > 1.2$. The region of the transition, where the quantity $N^{-1}dE^{(int)}/dU^{(0)}$ experiences the most dramatic drop, becomes increasingly narrower with increasing polymer size N . Moreover, since the magnitude of the overall change in the specific energy slope also increases with N , the coil-to-globule transition becomes 'sharper' with N in the GSC theory, consistent with the MC simulation data and the transition being of second order^{14,13}. Note also, that the theta-point, which we may define e.g. as the point of the maximal change in $N^{-1}dE^{(int)}/dU^{(0)}$, shifts towards lower values of $U^{(0)}$ with increasing N .

V. CONCLUSION

In this paper we have developed a version of the Gaussian self-consistent (GSC_R) technique which does not rely on the virial-type expansion of the Hamiltonian in terms of powers of the density, $\rho \propto \langle r^{-L} \rangle$. As a result, it is now possible to apply the new method to practically any polymer model involving conventional molecular interactions.

Thus, we have been able to compare the mean spatial characteristics and the energy values between the results from the GSC theory and Monte Carlo (MC) simulation based on precisely the same model, which includes the harmonic bonded and the Lennard-Jones pairwise interactions. This comparison has been performed for three types of macromolecular architectures of an isolated chain: a ring, an open polymer, and a star. We have done this also across the range of the coil-to-globule transition, as well as for different degrees of polymerisation and degrees of flexibility. Naturally, the GSC theory agrees with the second order nature of the coil-to-globule transition for flexible homopolymers.

Importantly, the speed of numeric computation is much faster²⁹ in the GSC method than in the equivalent MC simulation for obtaining the same data, particularly so for systems possessing an extra kinematic symmetry, such as for rings or stars.

Overall, the agreement in the shapes of the curves and many of the particular numerical values of observables between GSC and MC is better than one could have anticipated given the relative simplicity of the GSC technique. Where any significant level of deviation does occur, it has been identified as either related to the correlation hole effect at small separations, or to the stretched Gaussian behaviour at large separations, in the radial distribution function (RDF)²⁴.

In particular, for the repulsive coil, the energy and the mean squared distances between near monomers along the chain are quite accurate in the GSC theory as compared to the MC data (with a typical deviation of several percent), but the distances between remote monomers, and hence the radius of gyration, are overestimated by the GSC method (with a typical deviation of a few dozen percent). This is a well known drawback of such a theory, related to the overestimation of the Flory swelling exponent for long chains, due to the fact that the RDF here does

not have a stretched exponential behaviour at large separations. On the contrary, for a rather stiff coil, the GSC theory underestimates the radius of gyration. This may be due to shortcomings of the hard sphere Camahan{Starling term. For the collapsed globule, on the other hand, the distances and the radius of gyration are quite accurate in the GSC theory, although the mean energy is less so because of the lack of a sharp liquid-like peak in the RDF.

To make the agreement of GSC and MC better, one has to finally overcome the most restrictive feature of the method – the Gaussian shape of RDF itself. One possible way of doing this is to take a linear superposition of the Gaussian trial functions, thereby permitting ‘stretching’ of the Gausoid. This should be sufficient for curing the problem with the swelling exponent of the repulsive coil in the GSC theory. Work along these lines is currently in progress. The main difficulties in doing this are in the considerable mathematical complications when calculating the non-Gaussian conformational entropy of the chain, as well as in the added numerical complexity, since a radial mesh for RDF would have to be introduced. Nevertheless, we intend to resolve these issues and hope to present a more accurate, and at last a non-Gaussian self-consistent theory in the near future.

ACKNOWLEDGMENTS

The authors are grateful for interesting discussions to Professor F. Ganazzoli, Professor H. Orland, Dr G. Raos, Dr T. Garel, and to R. Connolly for his help. The support of the Enterprise Ireland international collaboration grants IC/2001/074 and BC/2001/034, as well as the IRCSET basic research grant SC/02/226 are also acknowledged.

-
- ¹ E. G. Timoshenko, Yu. A. Kuznetsov, K. A. Dawson. *Phys. Rev. E* 57 6801 (1998).
 - ² F. Ganazzoli. *J. Chem. Phys.* 108 9924 (1998).
 - ³ F. Ganazzoli. *J. Chem. Phys.* 112 1547 (2000).
 - ⁴ Yu. A. Kuznetsov, E. G. Timoshenko. *J. Chem. Phys.* 111 3744 (1999).
 - ⁵ F. Ganazzoli, R. La Ferla, G. Allegra. *Macromol.* 28 5285 (1995).
 - ⁶ R. R. Netz, H. Orland. *Eur. Phys. J.* 8 81 (1999).
 - ⁷ Yu. A. Kuznetsov, E. G. Timoshenko, K. A. Dawson. *J. Chem. Phys.* 104 3338 (1996).
 - ⁸ E. G. Timoshenko, Yu. A. Kuznetsov, K. A. Dawson. *J. Chem. Phys.* 102 1816 (1995).
 - ⁹ F. Ganazzoli, Yu. A. Kuznetsov, E. G. Timoshenko. *Macromol. Theory Simul.* 10 325 (2001).
 - ¹⁰ F. Ganazzoli, R. La Ferla. *J. Chem. Phys.* 113 9288 (2000); F. Ganazzoli, R. La Ferla, G. Ragaini. *Macromol.* 34 4222 (2001).
 - ¹¹ Yu. A. Kuznetsov, E. G. Timoshenko. *IL Nuovo Cimento* 20D (12bis) 2265 (1998).
 - ¹² E. G. Timoshenko, Yu. A. Kuznetsov. *J. Chem. Phys.* 112 8163 (2000).
 - ¹³ M. Doi, S. F. Edwards. *The Theory of Polymer Dynamics*. Oxford Science. New York (1989).
 - ¹⁴ J. des Cloizeaux, G. Jannink. *Polymers in Solution*. Oxford Science Publ (1990).
 - ¹⁵ S. F. Edwards, P. Singh. *J. Chem. Soc. Faraday Trans. II* 75 1001 (1979).
 - ¹⁶ J. des Cloizeaux. *J. de Physique* 31 715 (1970).
 - ¹⁷ E. Pitard, H. Orland. *Europhys. Lett.* 41 467 (1998).
 - ¹⁸ E. Pitard. *Eur. Phys. J. B* 7 665 (1999).
 - ¹⁹ H. H. Gan, B. C. Eu. *J. Chem. Phys.* 99 4084 (1993); *ibid* 4103 (1993).
 - ²⁰ M. P. Taylor, J. E. G. Lipson. *J. Chem. Phys.* 104 4835 (1996); 106 5181 (1997).
 - ²¹ G. Allegra, F. Ganazzoli. *J. Chem. Phys.* 83 397 (1985).
 - ²² G. Allegra, E. Colombo, F. Ganazzoli. *Macromol.* 26 330 (1993).
 - ²³ G. Raos, G. Allegra, F. Ganazzoli. *J. Chem. Phys.* 100 7804 (1994).
 - ²⁴ E. G. Timoshenko, Yu. A. Kuznetsov, R. Connolly. *J. Chem. Phys.* 116 3905 (2002).
 - ²⁵ J.-P. Hansen, I. R. McDonald. *Theory of simple liquids*. Academic Press, London (1990).
 - ²⁶ N. F. Camahan, K. E. Starling. *J. Chem. Phys.* 51 635 (1969).
 - ²⁷ V. Talanquer, D. W. Oxtoby. *Faraday Discuss.* 112 91 (1999); M. Robles, M. L. de Haro. *Phys. Chem. Chem. Phys.* 3 5528 (2001).
 - ²⁸ E. G. Timoshenko, Yu. A. Kuznetsov. *Colloids and Surfaces A* 190 135 (2001).
 - ²⁹ Benchmarks were performed on an AMD Athlon MP 1900+ with the following run time parameters. For the ring: MC: S = 50;000, t = 8 N², resulting in the total run time t_{total} = 1000 minutes; GSC: n_{iterations} = 5;000, resulting in t_{total} < 1 minute. For the open chain: MC: S = 50;000, t = 40 N², resulting in t_{total} = 5;000 minutes; GSC: n_{iterations} = 18;000, resulting in t_{total} = 25 minutes.

³⁰ R. Guida, J. Zinn (Justin, J. Phys. A 31 8103 (1998)).

FIGURE CAPTIONS

FIG .1. Plots of the half(ring radial distribution functions $g_{0N=2}^{(2)}(r)$ (in \AA^3 units) from MC (solid thick lines) and the GSC theory with $a = 0.9$ (thin dashed lines) vs the radial separation r (in \AA units) for the flexible ring homopolymers with $\nu = 0$ and $\nu = 1$. The main part of the figure corresponds to the good solvent $U^{(0)} = 0$ and the polymer size $N = 300$, whereas the inset corresponds to the poor solvent $U^{(0)} = 6$ and the polymer size $N = 200$.

FIG .2. The mean(squared distances D_{0k} (in \AA^2 units) of an open flexible homopolymer with $N = 200$, $\nu = 0$, and $\nu = 1$ in the good solvent, $U^{(0)} = 0$, vs the chain index k . Here and below the solid thick lines correspond to the MC data, the solid thin lines to the GSC theory with $a = 1.0$, and the dashed lines to the GSC theory with $a = 0.9$.

FIG .3. The mean(squared distances D_{0k} (in \AA^2 units) of a fairly flexible, $\nu = 1$, ring homopolymer with $N = 300$ and $\nu = 1$ in the good solvent, $U^{(0)} = 0$, vs the chain index k .

FIG .4. The mean(squared distances D_{0k} (in \AA^2 units) of a semiflexible, $\nu = 5$, ring homopolymer with $N = 300$ and $\nu = 1$ in the good solvent, $U^{(0)} = 0$, vs the chain index k .

FIG .5. The mean(squared distances D_{0k} (in \AA^2 units) from the core monomer of a flexible, $\nu = 0$, homopolymer star with $f = 12$ arms, $\nu = 1$, and the arm length $N_{\text{arm}} = f = 50$ in the good solvent, $U^{(0)} = 0$, vs the chain index k .

FIG .6. The mean(squared distances D_{0k} (in \AA^2 units) for the globule of a flexible, $\nu = 0$, ring homopolymer with $N = 200$, $\nu = 1$, and $U^{(0)} = 6$ vs the chain index k .

FIG .7. The mean(squared radius of gyration $3R_g^2$ (in \AA^2 units) of a flexible, $\nu = 0$, homopolymer ring with $N = 150$ and $\nu = 1$ vs the dimensionless degree of the Lennard-Jones attraction, $U^{(0)}$, across the coil-to-globule transition.

FIG .8. The mean energy $E^{(\text{int})}$ (in $k_B T$ units) of a flexible, $\nu = 0$, homopolymer ring with $N = 150$ and $\nu = 1$ vs the degree of the Lennard-Jones attraction, $U^{(0)}$, across the coil-to-globule transition.

FIG .9. Plots of the specific energy slope, $N^{-1} dE^{(\text{int})}/dU^{(0)}$, (in $k_B T$ units) of flexible, $\nu = 0$, homopolymer rings with $\nu = 1$ vs the degree of the Lennard-Jones attraction, $U^{(0)}$, across the coil-to-globule transition for different polymer sizes $N = 50; 100; 200; 300$ (from top to bottom). These are obtained from the GSC theory with $a = 0.9$.

T A B L E S

TABLE I. Comparison of the mean energy values $E^{(int)}$ (in $k_B T$ units) for different homopolymers from the MC simulation (second column) based on the data set of Ref.²⁴ and from the GSC theory with the parameter $a = 0.9$ (third column) and $a = 1.0$ (fourth column). The fifth and sixth columns contain the relative deviation $\delta = (E^{(int)}(GSC) - E(MC)) / E(MC) \cdot 100\%$ for these two cases given as a percentage. The model parameters, which are suppressed within the tables, such as e.g., $U^{(0)}$, are equal to zero.

System	MC	GSC, $a = 0.9$	GSC, $a = 1.0$	$a = 0.9; \%$	$a = 1.0; \%$
Ring, $N = 100$					
$\phi = 0.01$	148.6	148.58	148.59	0	0
$\phi = 0.1$	151.21	151.22	151.51	0	0.2
$\phi = 0.2$	155.24	155.52	156.22	0.2	0.6
$\phi = 0.5$	168.3	170.03	172.0	1.0	2.2
$\phi = 2.0$	232.4	232.1	239.0	0.1	2.8
Ring, $\phi = 1$					
$N = 50$	94.76	96.08	97.99	1.4	3.4
$N = 100$	190.4	193.1	196.9	1.4	3.4
$N = 200$	381.5	386.9	394.4	1.4	3.4
$N = 300$	572.6	580.6	591.9	1.4	3.4
Open, $\phi = 1$					
$N = 150$	284.2	287.1	292.7	1.0	3.0
$N = 200$	378.7	383.9	391.3	1.4	3.3
Semi-flexible Ring $\phi = 1; \phi = 1$					
$N = 50$	106.6	104.9	107.3	1.6	0.7
$N = 100$	213.3	210.2	215.1	1.4	0.8
$N = 200$	426.8	420.9	430.7	1.4	0.9
$N = 300$	640.2	631.6	646.2	1.3	0.9
Semi-flexible Ring $\phi = 5; \phi = 1$					
$N = 50$	110.1	110.5	113.2	0.4	2.8
$N = 100$	218.6	220.5	225.7	0.9	3.2
$N = 200$	436.2	440.9	451.4	1.1	3.5
$N = 300$	653.9	661.4	677.0	1.1	3.5
Star, $N=f=50; \phi = 1$					
$f = 3$	286.5	295.1	301.2	3.0	5.1
$f = 6$	575.1	596.5	608.8	3.7	5.9
$f = 9$	864.8	902.1	920.8	4.3	6.5
$f = 12$	1156.	1211.	1236.	4.7	6.9
Globule of a Ring $U^{(0)} = 6; \phi = 1$					
$N = 100$	426.7	287.2	211.9	32.7	50.3
$N = 200$	1000.	722.6	540.3	27.7	46.0

TABLE II. Comparison of the mean squared radius of gyration values $3R_g^2$ (in σ^2 units) for different homopolymers from the MC simulation (second column) based on the data set of Ref.²⁴ and from the GSC theory with the parameter $a = 0.9$ (third column) and $a = 1.0$ (fourth column). The fifth and sixth columns contain the relative deviation $= (R_g^2(\text{GSC}) - R_g^2(\text{MC}) / R_g^2(\text{MC}) \cdot 100\%$ for these two cases given as a percentage.

System	MC	GSC, $a = 0.9$	GSC, $a = 1.0$	$a = 0.9; \%$	$a = 1.0; \%$
Ring, $N = 100$					
$\phi = 0.01$	2497.	2503.6	2504.6	0.3	0.3
$\phi = 0.1$	273.57	275.18	277.8	0.6	1.5
$\phi = 0.2$	153.56	157.61	160.81	2.6	4.7
$\phi = 0.5$	82.68	91.04	94.69	10.1	14.5
$\phi = 2.0$	45.98	60.70	64.84	32.0	41.0
Ring, $\phi = 1$					
$N = 50$	26.66	28.90	30.32	8.4	13.7
$N = 100$	61.45	70.30	74.16	14.4	20.7
$N = 200$	141.4	172.3	182.7	21.8	29.2
$N = 300$	232.4	292.0	310.3	25.6	33.5
Open, $\phi = 1$					
$N = 150$	185.7	221.4	234.3	19.2	26.2
$N = 200$	253.5	321.6	341.0	26.9	34.5
Semi-flexible Ring $\phi = 1; \phi = 1$					
$N = 50$	37.91	38.18	40.71	0.7	7.4
$N = 100$	86.07	92.97	99.44	8.0	15.5
$N = 200$	193.6	222.9	239.0	15.1	23.5
$N = 300$	305.1	371.5	398.8	21.8	30.7
Semi-flexible Ring $\phi = 5; \phi = 1$					
$N = 50$	78.05	60.60	65.58	22.3	16.0
$N = 100$	210.8	161.0	175.8	23.6	16.6
$N = 200$	499.8	382.5	419.0	23.5	16.2
$N = 300$	861.3	622.0	681.5	27.8	20.8
Star, $N = f = 50; \phi = 1$					
$f = 3$	146.2	176.4	186.6	20.6	27.6
$f = 6$	185.2	239.0	253.1	29.0	36.7
$f = 9$	208.7	278.0	294.5	33.2	41.1
$f = 12$	228.7	308.1	326.5	34.7	42.8
Globule of a Ring $U^{(0)} = 6; \phi = 1$					
$N = 100$	6.126	6.431	7.384	5.0	20.5
$N = 200$	9.368	9.872	11.31	5.4	20.7

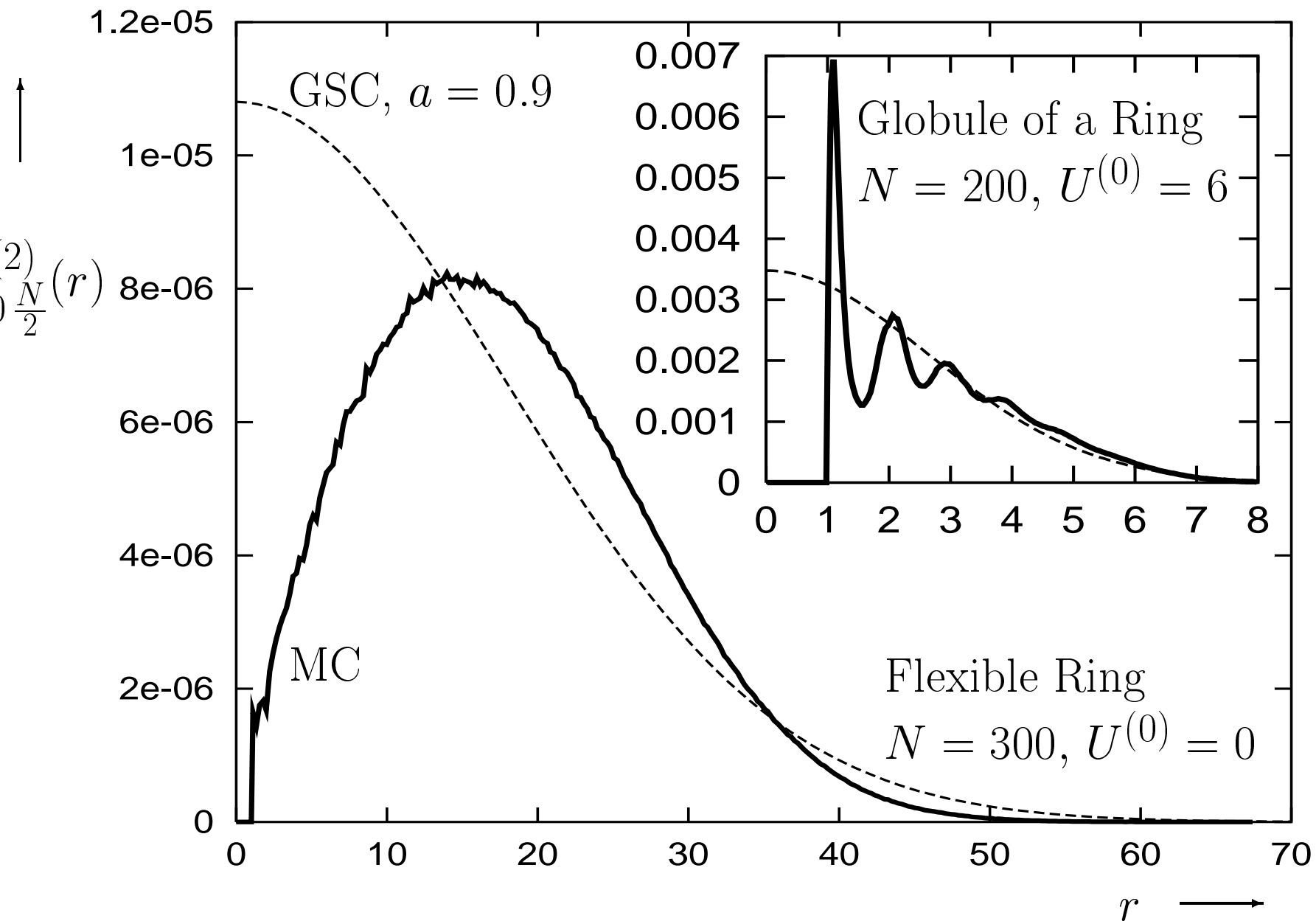


Fig. 1

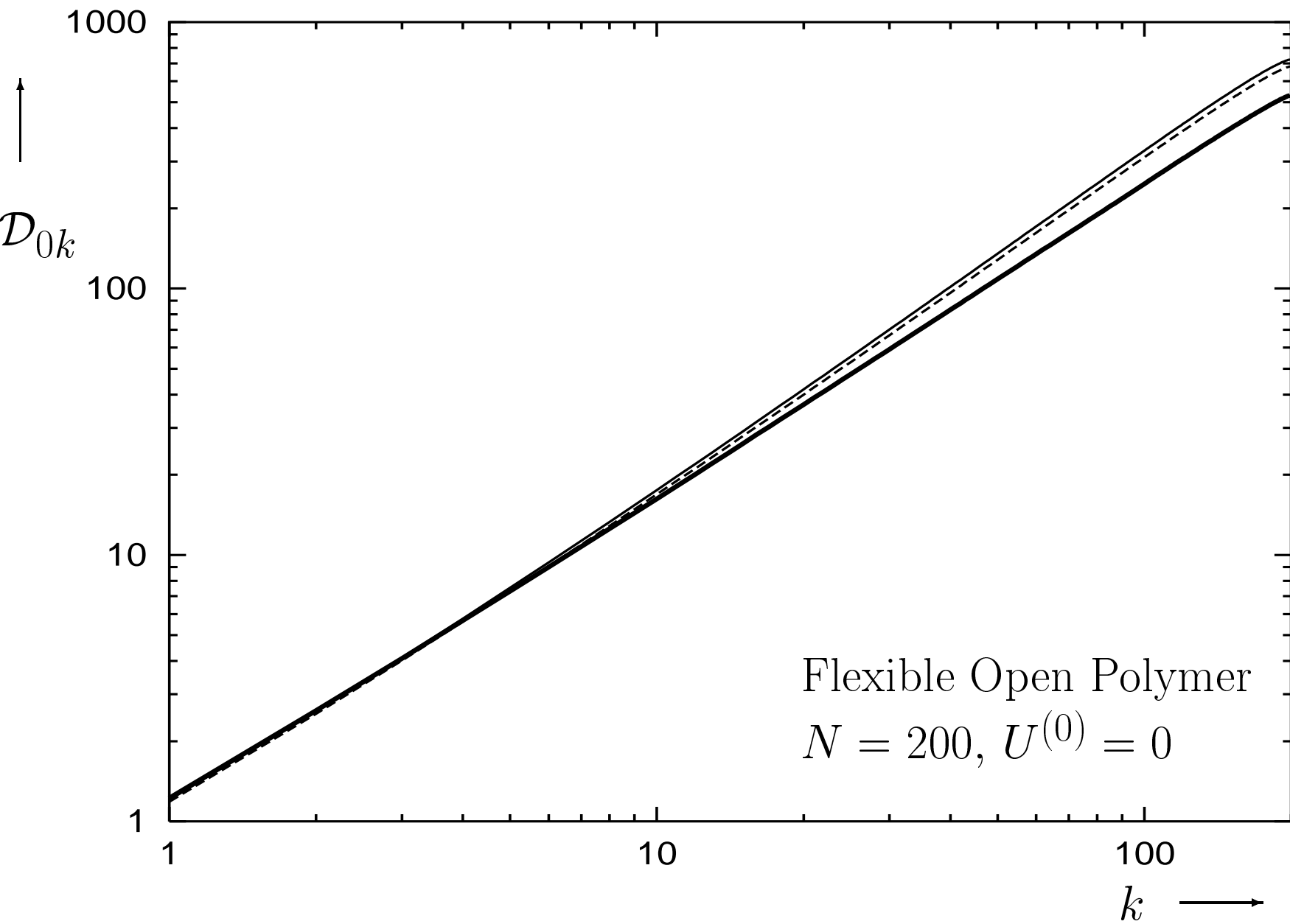


Fig. 2

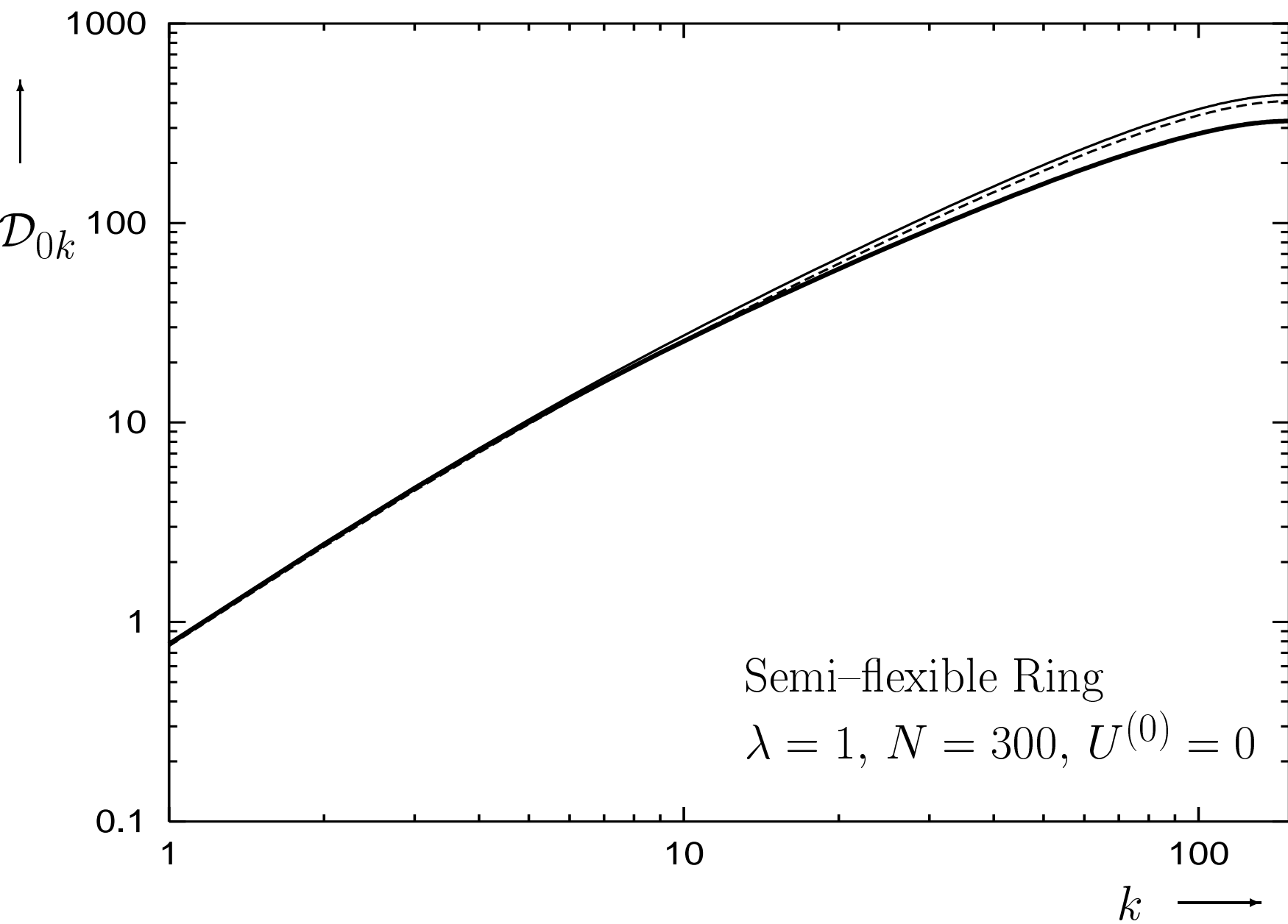


Fig. 3

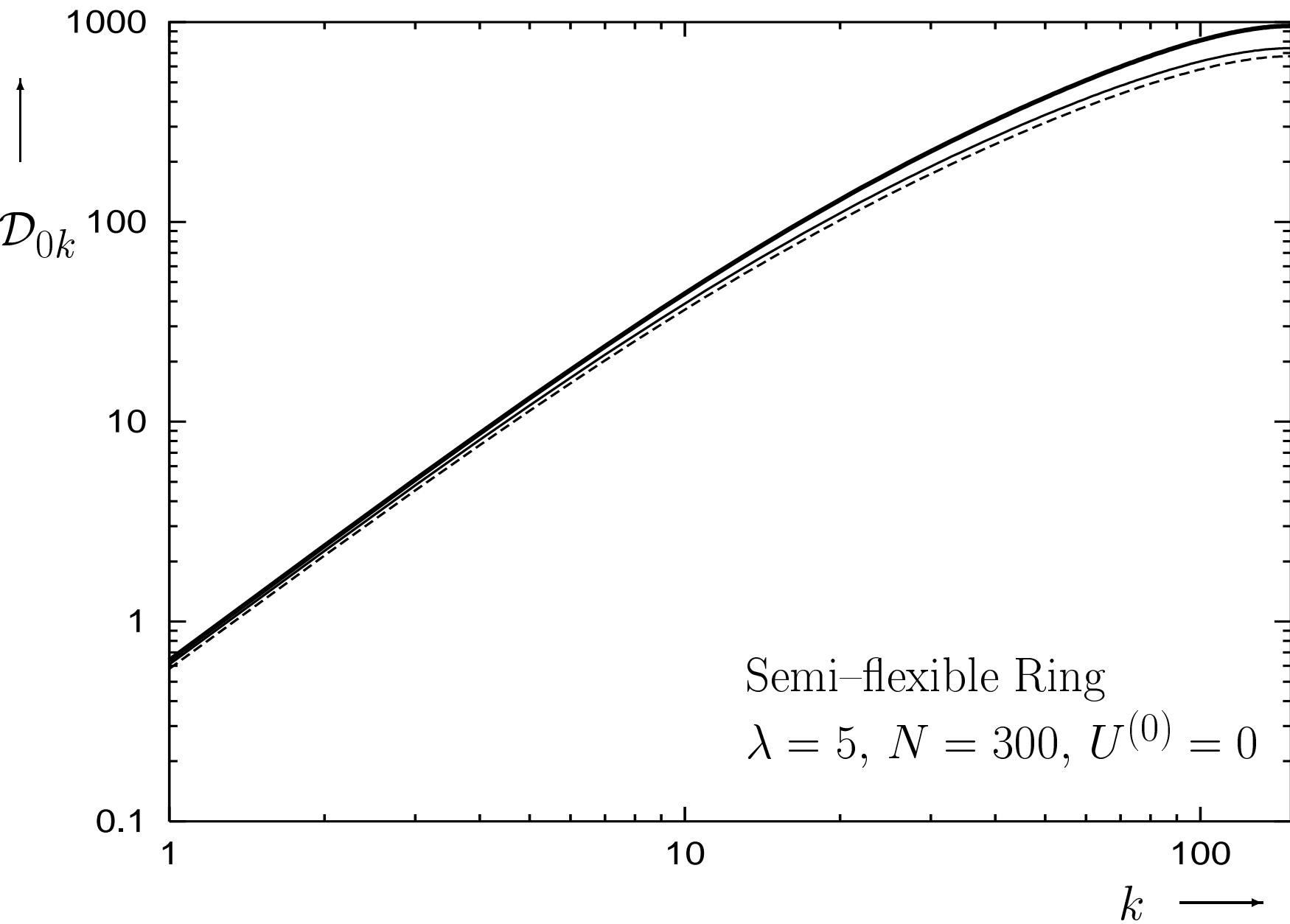


Fig. 4

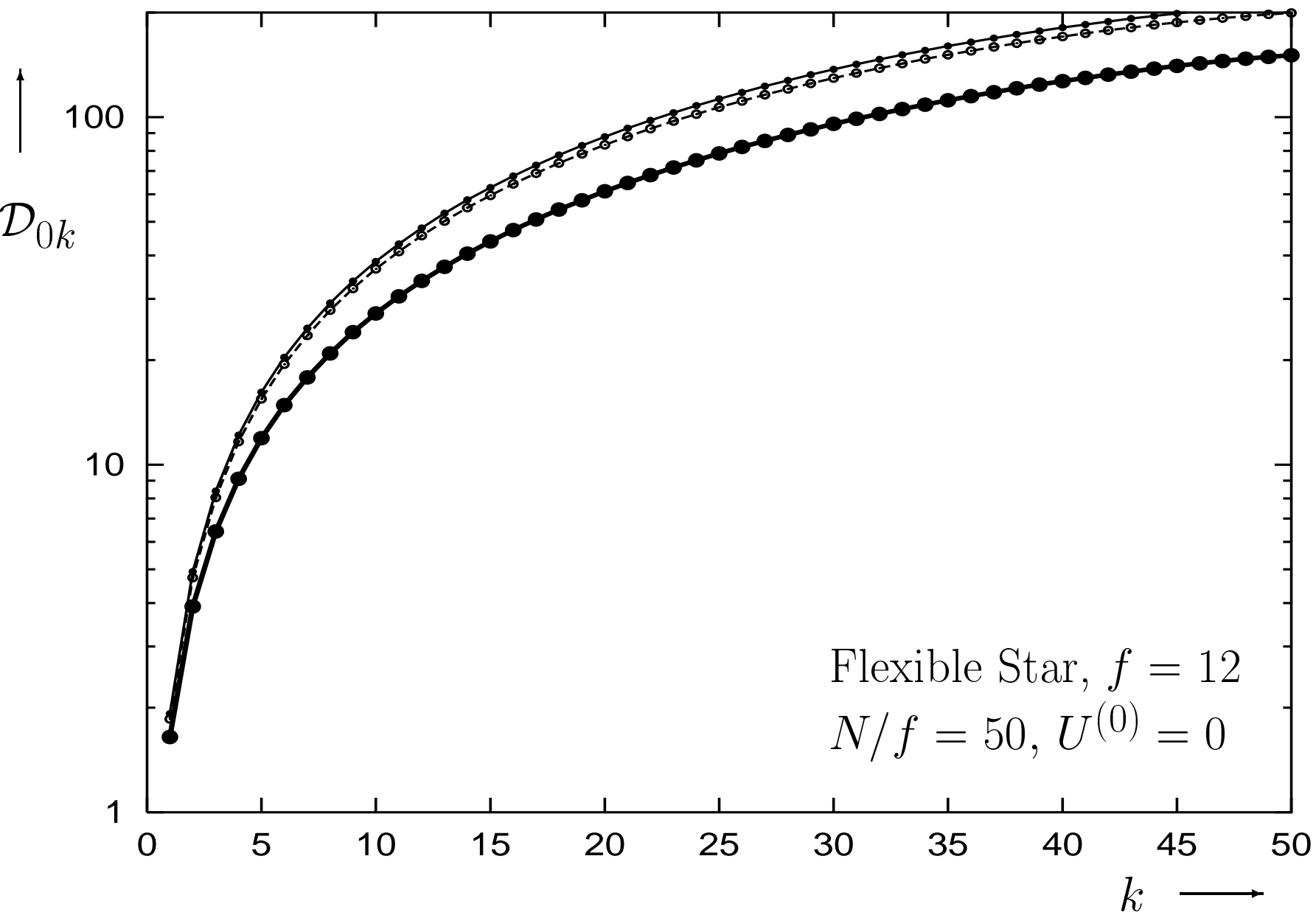


Fig. 5

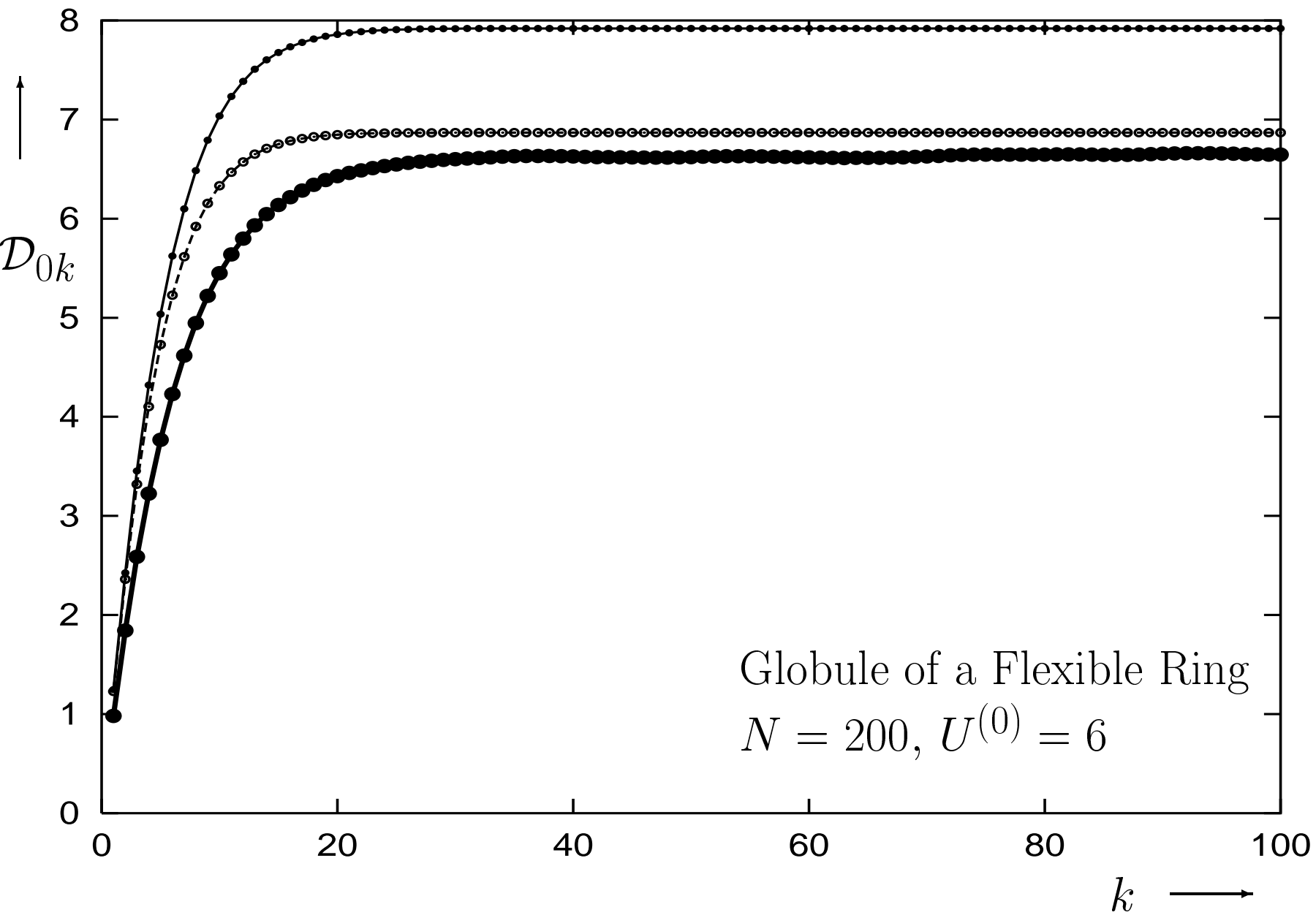


Fig. 6

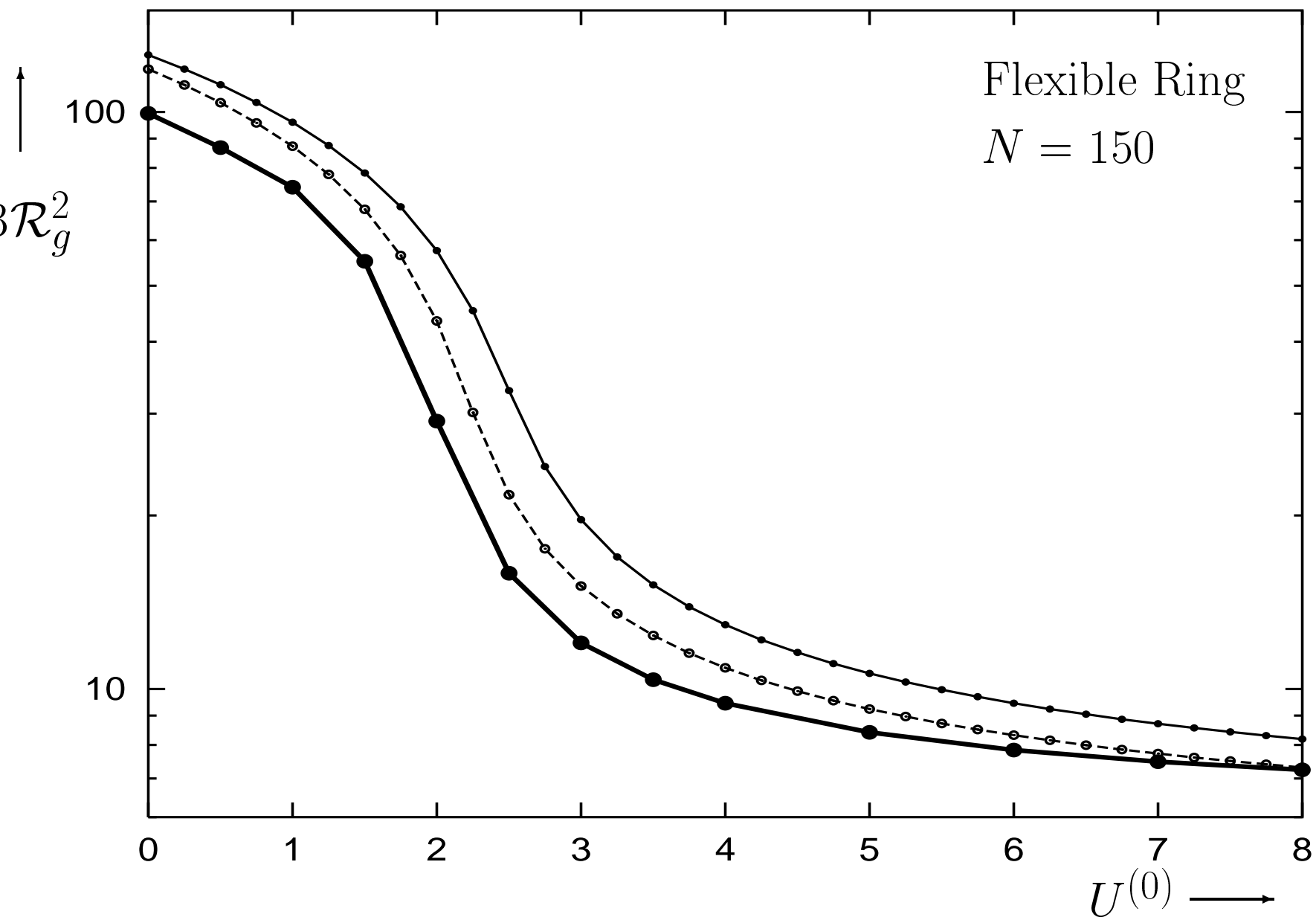


Fig. 7

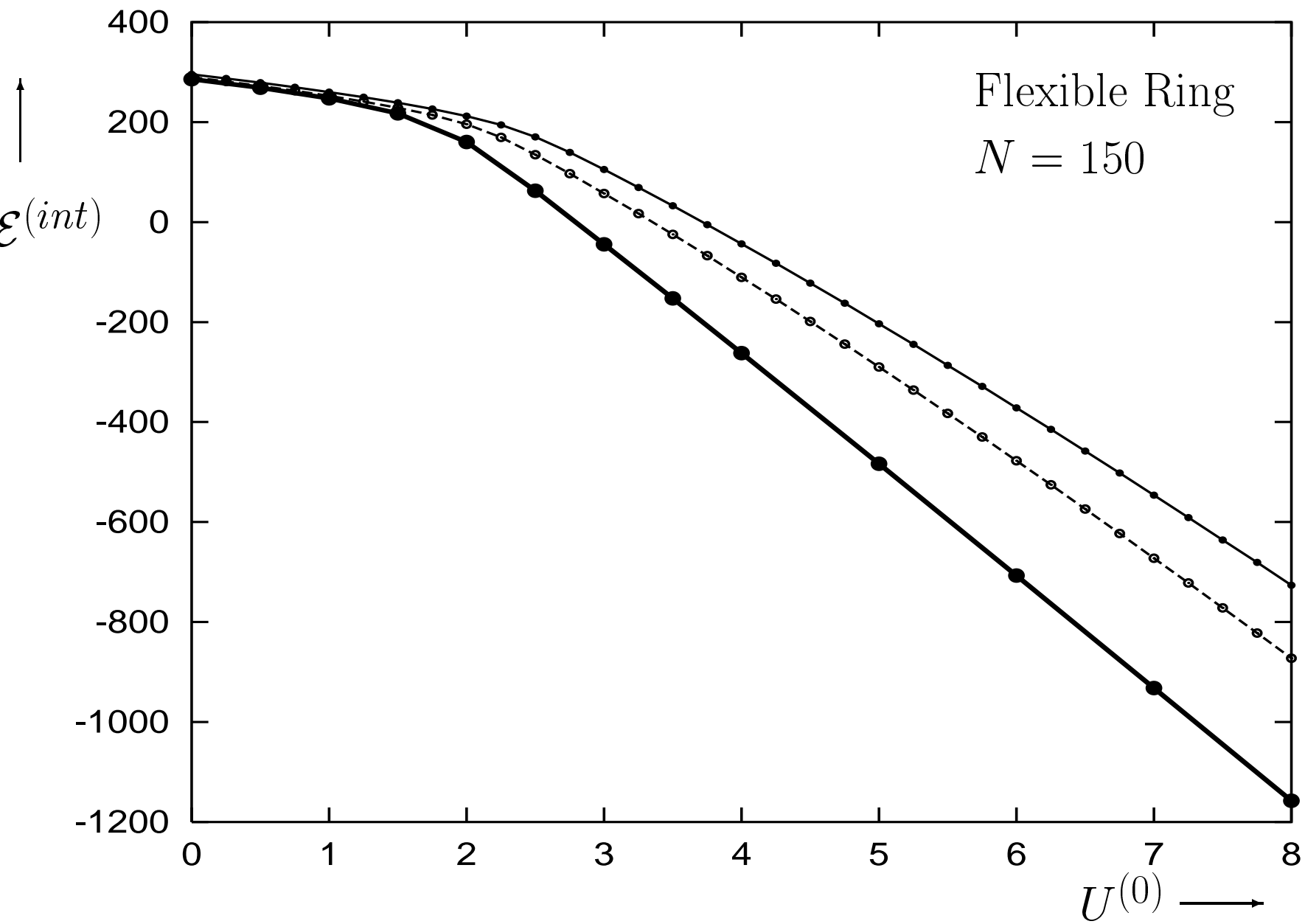


Fig. 8

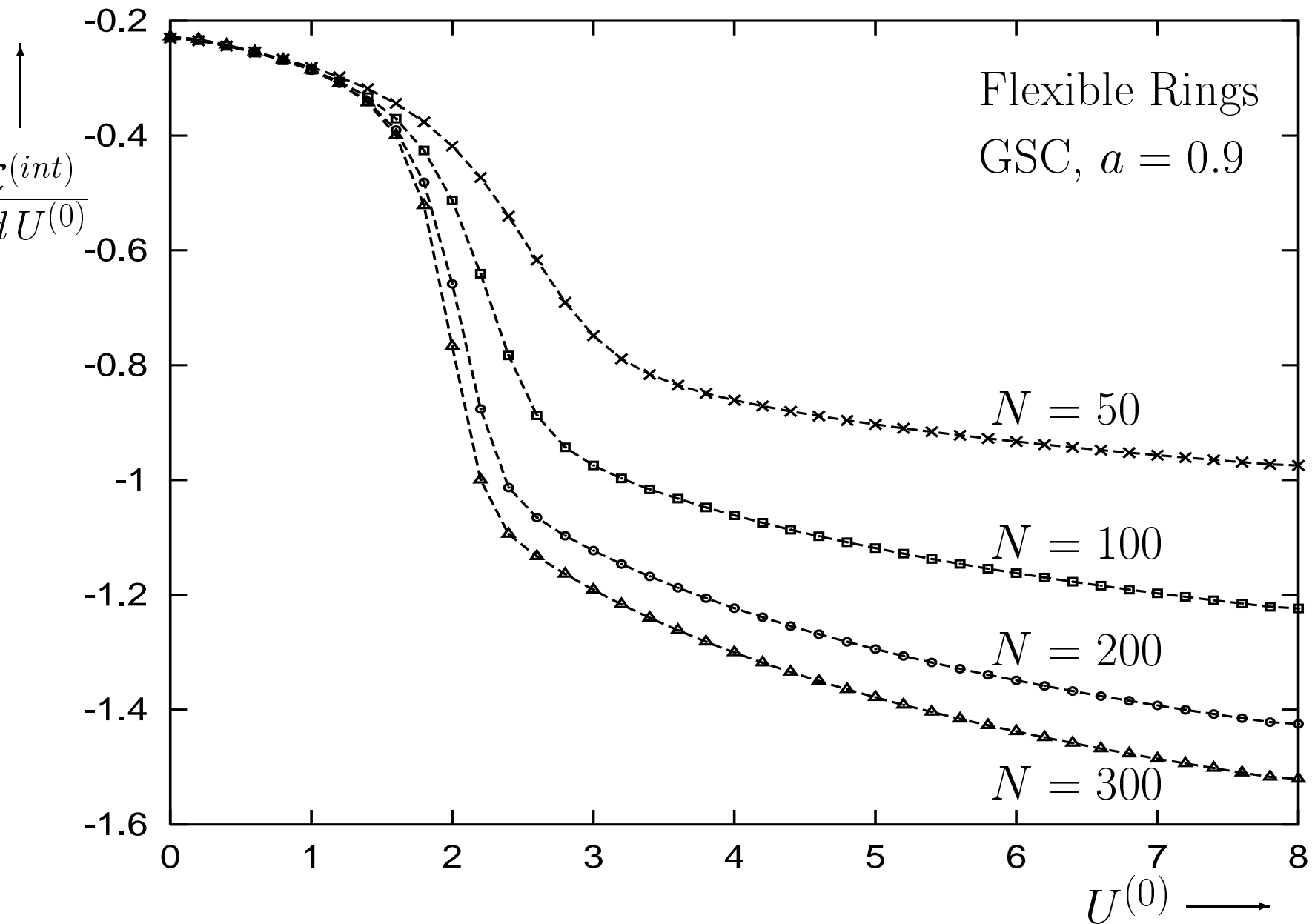


Fig. 9